

Contents

1	Theory.	3
2	PHENIX Apparatus and Event Recontruction.	5
3	Electron Identification.	7
3.1	Parameters used for electron selection.	8
3.1.1	RICH Parameters	8
3.1.2	EmCal Parameters	9
3.2	Background sources	12
3.3	Data Set and Quality Selection.	15
3.3.1	Beam conditions	16
3.3.2	Magnetic Field Stability	17
3.3.3	Electron Identification parameters check.	18
3.3.4	Acceptance - Efficiency check.	19
3.3.5	QA Summary	21
3.4	Parameters Calibration	22
3.4.1	Momentum	22
3.4.2	RICH Mirror Alignment	22

3.4.3	EmCal matching	22
3.4.4	<i>dep</i>	22
3.5	Electron Selection Optimization.	22
4	Acceptance and Efficiency Estimation.	27
4.1	PHENIX Monte Carlo Simulation : PISA	28
4.2	Conversion Electrons.	29
4.3	Tuning the PISA	31
4.3.1	eID Tuning	31
4.3.2	Dead Areas Implementation	31
4.4	J/ψ Acceptance \times Efficiency Calculation	31
4.5	Particle Multiplicity Dependence	31
5	Measurement of J/ψ Production.	33
6	Results Interpretation.	35

List of Figures

3.1	Schematic of the Cherenkov radiation acquisition in RICH. . .	9
3.2	EmCal response to test beams of pions, protons and electrons.[2]	11
3.3	<i>dep</i> distribution for particle tracks in Au + Au collisions matching EmCal clusters in $3\sigma_{pos}$ (blue line) and the fraction of them which produces Cherenkov ring in RICH (red line). Their ratio is shown as a black line.	13
3.4	Estimation of number of electrons from a <i>dep</i> distribution. . .	14
3.5	“Radiograph” of $\gamma \rightarrow e^+e^-$ decay sources at PHENIX. Plot obtained from PHENIX Monte Carlo simulation when we introduce 50K simulated π^0 s.	16
3.6	Mean Beam Z vertex <i>versus</i> run number observed by BBC during Au + Au (left plot) and <i>p+p</i> run (right plot). Error bars are the RMS of vertex distribution.	17
3.7	Average momentum of all charged particles in east and west spectrometer arms <i>versus</i> run number during Au + Au and <i>p+p</i> collision periods. All tracks have hits in three DCH planes and matches PC1 and EmCal clusters.	18

3.8	Run number dependences of electron identification parameters used in heavy vector mesons analysis. The red points are run number rejected for further analysis.	24
3.9	Run dependence of electron yield. The top panels shows yields for each spectrometer arm. The bottom panels shows the product obtained from both arms. The Au + Au and $p+p$ runs were split in acceptance groups. The horizontal lines are the average of each group. Gray open circles correspond to rejected runs.	25
4.1	PHENIX Monte Carlo setup and the response to a generated J/ψ . Electrons are represented by red lines. Cherenkov photons are black lines. RICH structure is not drawn for clarity. .	28
4.2	Invariant mass spectrum of $\gamma \rightarrow e^+e^-$ conversion in beam pipe.	30

List of Tables

3.1	Data set obtained during Au + Au and $p+p$ Runs for different triggers.	17
3.2	Data set after quality selection.	22

Introduction

Chapter 1

Theory.

Chapter 2

PHENIX Apparatus and Event Recontruction.

Chapter 3

Electron Identification.

In this chapter we discussed the procedure for electron identification at PHENIX. For simplicity, when we mention electrons we are including positrons. One of the major advantages in PHENIX is its capability to distinguish electrons in an environment 100 times more abundant in hadrons. The detectors dedicated for electron identification are RICH (??) and EmCal (??). The information obtained from Cherenkov rings and electromagnetic showers from these detectors are calibrated and optimized in order to return the best signal significance for our vector meson measurements. Here we also discuss how to ensure the quality of our data before the signal counting.

3.1 Parameters used for electron selection.

3.1.1 RICH Parameters

The primary criterion for electron identification is the RICH response to the particle crossing its volume. The particle track is projected on the phototube (PMT) wall according to the mirror alignment (fig. 3.1). We define the ring area $A0$ of radii $3.8 \text{ cm} < R < 8.4 \text{ cm}$ around the track projected. We also define a wider area $A1$ with maximum radii at 11.0 cm . The signal measured by each PMT is npe_i . The parameters we use are :

$\mathbf{n0} = \sum_i^{A0} |npe_i > npe_{ped}|$ number of PMTs with amplitude above a known background npe_{ped} inside $A0$

$\mathbf{npe0} = \sum_i^{A0} npe_i$ is the total signal measured by all PMTs in $A0$

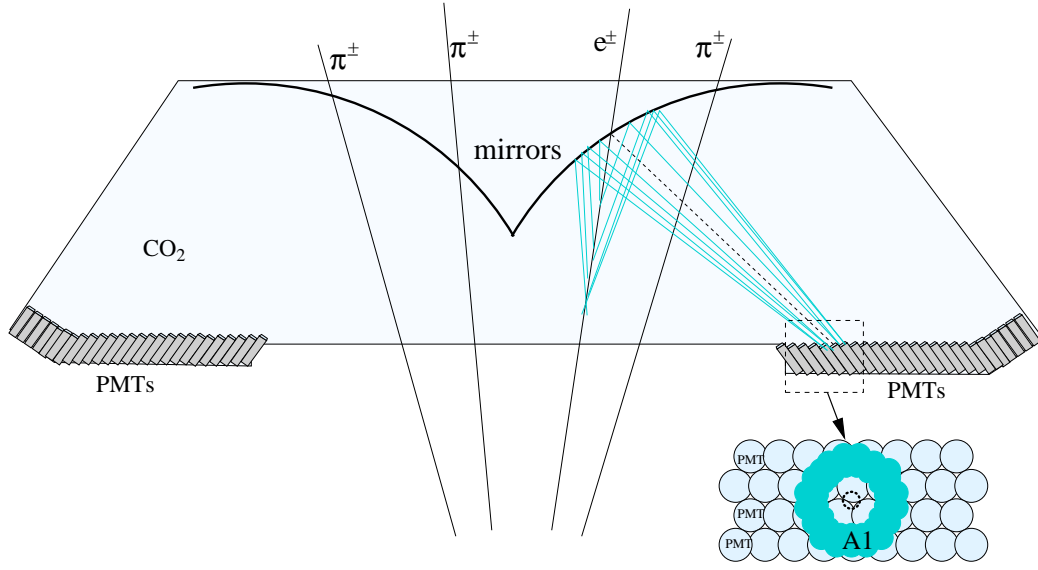


Figure 3.1: Schematic of the Cherenkov radiation acquisition in RICH.

$\mathbf{disp} = \left| \sum_i^{A0} (npe_i * \vec{x}_i) / npe0 - \vec{x}_{track} \right|$ distance between gravity center of ring and track projection \vec{x}_{track}

$\chi_{ring}^2 = \sum_i^{A0} ((R_i - R_0)^2 * npe_i) / npe0$ is the χ^2 of a ring with radii $R_0 = 5.9$ cm fitted to fired PMTs with distance R_i to the gravity center

$\mathbf{n1}$ number of PMTs with amplitude above a known background inside A1

$\mathbf{npe1}$ total signal measured by the PMTs in A1

3.1.2 EmCal Parameters

The amount of material from the vertex axis to EmCal is 0.4% in unities of radiation length X_0 . Photons coming from π^0 s and direct γ s convert in e^+e^- pairs when cross this material and pass the RICH criteria. In order to

reject electrons coming out of the vertex axis, we use the matching between the particle track and EmCal energy cluster

$emcsdphi_e = (\phi_{proj.track} - \phi_{en.cluster}) / \sigma_{pos}$ is the distance between the particle $\phi_{proj.track}$ projection on EmCal and energy cluster $\phi_{en.cluster}$ coordinate in unities of EmCal position resolution σ_{pos} considering electromagnetic shower

$emcsdz_e = (Z_{proj.track} - Z_{en.cluster}) / \sigma_{pos}$ is the distance between the particle $Z_{proj.track}$ projection on EmCal and energy cluster $Z_{en.cluster}$ coordinate in unities of EmCal position resolution σ_{pos} considering electromagnetic shower

In the section 3.4.3 we discuss all dependences of this parameter.

Electrons deposit all their kinematic energy into the EmCal while hadrons leave only a fraction of their energy (fig. 3.2). We take advantage of this property by using the energy E in the cluster associated to the particle track with momentum P and we obtain

$$\mathbf{dep} = \frac{E - P}{P} \frac{1}{\sigma_E(E/P)} \quad (3.1)$$

where $\sigma_E(E/P)$ is the resolution of E/P measurement. The resolution is a function of momentum. We discuss the calibration of this parameter in the section 3.4.4.

The particle shower shape inside EmCal has distinguished properties for electrons and hadrons. We can use it in our electron selection. The energy

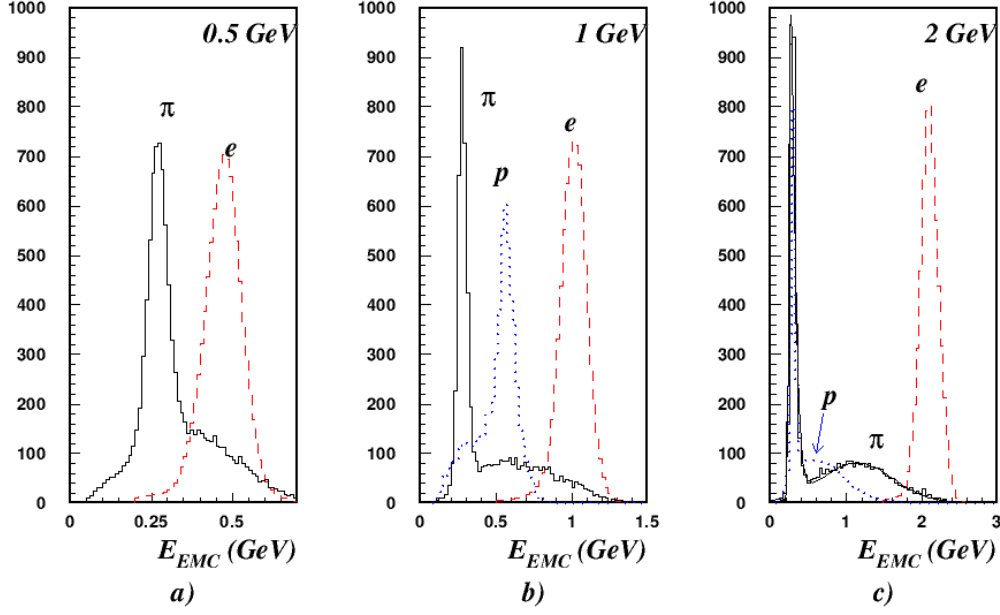


Figure 3.2: EmCal response to test beams of pions, protons and electrons.[2]

distribution shape expected for an electromagnetic shower is parameterized for every energy cluster. We obtain

$$\chi_{el}^2 = \sum_i \frac{[E_i^{measured} - E_i^{model}(x, \vec{a})]^2}{\sigma^2} \quad (3.2)$$

where $E_i^{measured}$ is the energy measured by the tower i and E_i^{model} is the energy expected for an electromagnetic shower with free parameters \vec{a} and distance x to the gravity center of the cluster. The model is independent of the total energy and particle incidence angle. We use the χ_{el}^2 probability *prob* as our selection criterion.

The figure 3.3 shows the dep distribution with and without RICH selection criteria in Au + Au collisions. It is clear the peak formed around zero when the RICH parameters are used for electron selection. The amount of other particles have reduced by a factor of 100 with the RICH criteria set applied in this plot. But even with this selection the peak at dep around zero is sitting on a large background. Most of the background is naturally removed when we require minimum mass criteria in the invariant mass spectrum. But we need to estimate it to perform further quality analysis.

3.2 Background sources

The background observed mainly comes from miss-associated tracks. At high particle density environment the tracks are easily associated to wrong Cherenkov rings. We can estimate this effect by making a dep distribution of miss-correlated tracks.

In the figure 3.4 we obtain the amount of electrons from a dep distribution. For each particle we associate it track with the closest Cherenkov ring, the standard procedure, and obtain the RICH parameters for that track. The selection using these parameters is the black line and includes signal+background. For the same particles we also associate it track with the closest Cherenkov ring but swapping the Z coordinate ($Z \rightarrow -Z$). We obtain swapped parameters from its associations and use the same selection criteria. It dep distribution (blue line) gives the miss-correlated background.

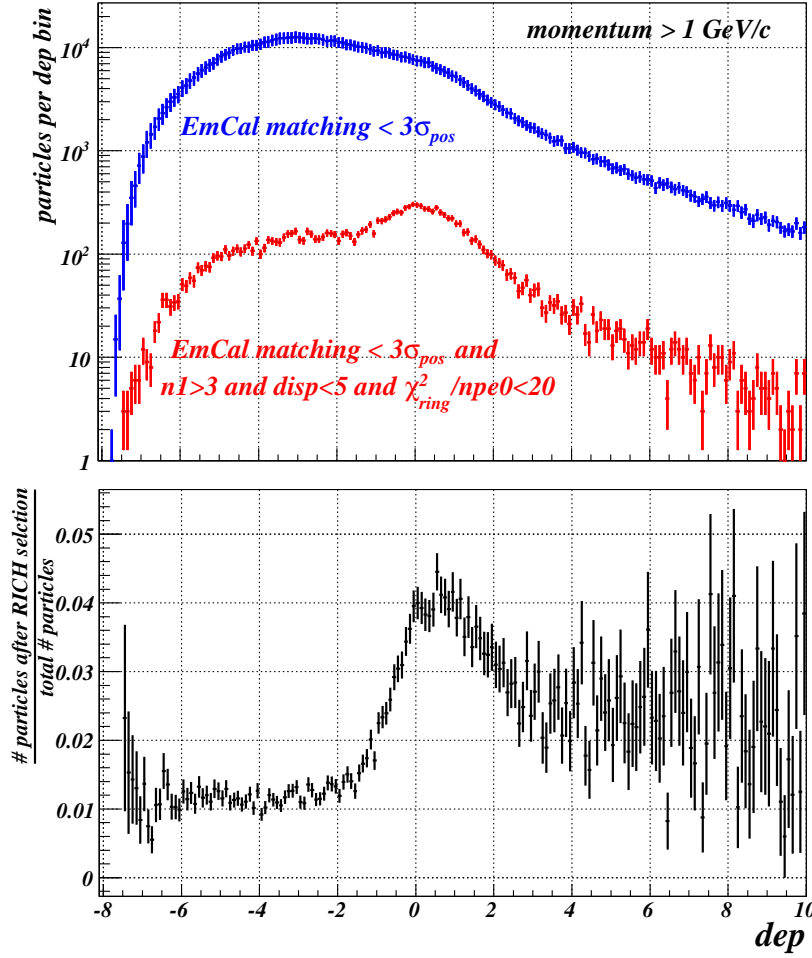


Figure 3.3: dep distribution for particle tracks in Au + Au collisions matching EmCal clusters in $3\sigma_{pos}$ (blue line) and the fraction of them which produces Cherenkov ring in RICH (red line). Their ratio is shown as a black line.

By subtracting the distributions we cleanup our electron distribution.

Hadrons can share a Cherenkov ring with an electron. The reflection of

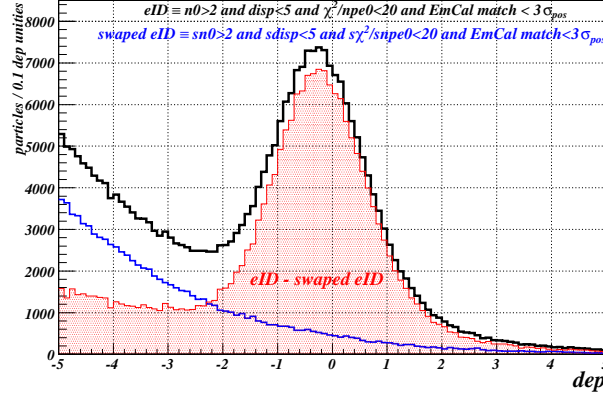


Figure 3.4: Estimation of number of electrons from a dep distribution.

parallel tracks on the spherical mirror project then in the same point on PMTs wall in RICH. If a pion track, for instance, is parallel to an electron it can share the same ring and be identified as an electron. We can use the post field open angle

$$\cos(\mathbf{pfoa}) = \left| \vec{A} \times \vec{B} \right| \quad (3.3)$$

between the particle directions \vec{A} and \vec{B} as a parameter to reject one of the tracks in this condition. For effect estimation usually we reject one of the electrons when they have $pfoa < 2.5$ degrees.

Noise and trips in DCH close to real particle tracks can be identified as additional particles by the tracking algorithm. We call these tracks “ghost” tracks. These tracks can also share Cherenkov rings and be misidentified. We reject one of the tracks when their distance each other is $\Delta phi < 0.02$ rad and $\Delta Z < 0.2$ cm at DCH. The track rejected is always that one with lowest $n0$. The second choice for rejection is the largest $disp$.

Another important source of electron sample background are electrons produced by γ s when they cross the detector material (beam pipe, RICH mirror, etc...). The figure 3.5 shows electrons produced into the PHENIX material according to detector Monte Carlo. The majority of these electrons are rejected by matching requirements, but if a converter electron is produced, i.e. in the beam pipe, its track is reconstructed as an electron from the collision point. Electrons produced at RHIC mirror, for instance, can have the same direction of normal pions and produce Cherenkov rings. The contribution of conversion electrons can be observed at subtracted dep distribution (fig. 3.4). They form the remaining background observed even after subtract the miss-correlated contribution.

3.3 Data Set and Quality Selection.

The Table 3.3 summarizes the amount of events obtained during Au + Au and $p+p$ Runs which we use in this work. These numbers were obtained from event scalers in the DAQ and include all sort of beam, magnetic field and material amount conditions. The data is labeled with run numbers for calibration and acquisition conditions control. In this step of analysis we define a set of quality analysis (QA) criteria to select run numbers with suitable conditions for heavy vector mesons analysis.

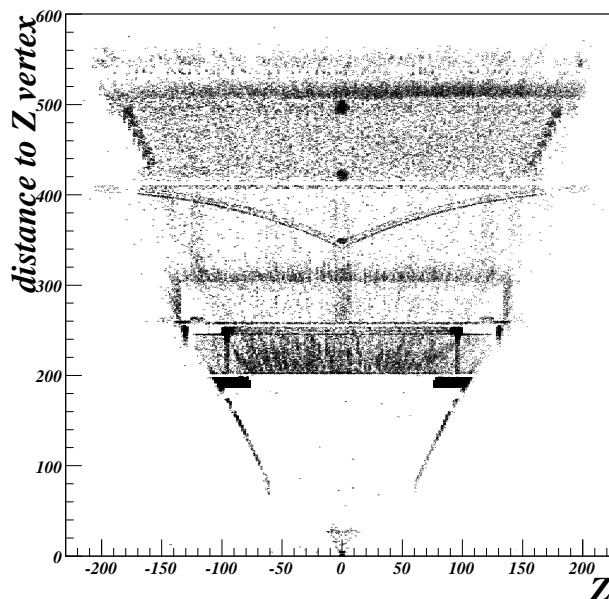


Figure 3.5: “Radiograph” of $\gamma \rightarrow e^+e^-$ decay sources at PHENIX. Plot obtained from PHENIX Monte Carlo simulation when we introduce 50K simulated π^0 s.

3.3.1 Beam conditions

The figure 3.6 shows the average Z vertex *versus* run number. In all electron analysis we accept collisions up to 30 cm far from the center of PHENIX at Z axis. All runs recorded were accept for analysis according to this QA criterion.

specie	events sampled	events recorded	Minimum Bias	ERT Electron	ERT 4x4C
Au + Au	6996M	1599M	1599M	0	0
$p+p$	89.5B	7110M	2260M	449.7M	1650B

Table 3.1: Data set obtained during Au + Au and $p+p$ Runs for different triggers.

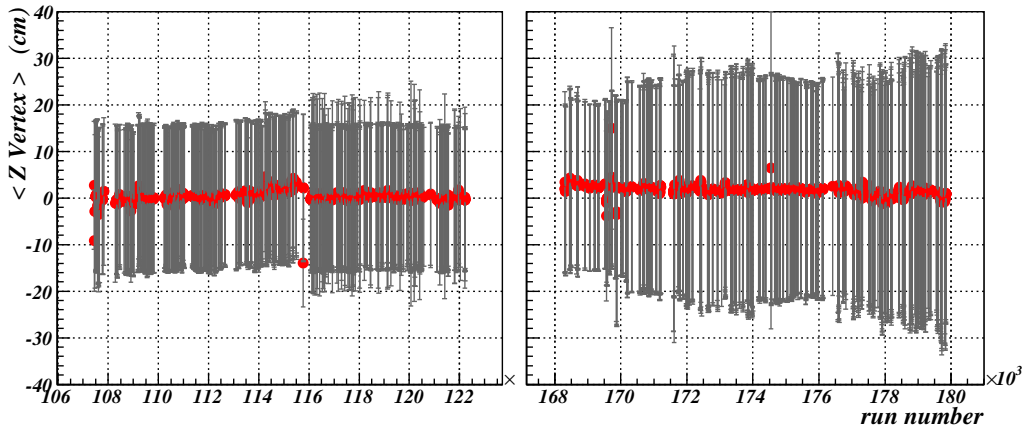


Figure 3.6: Mean Beam Z vertex *versus* run number observed by BBC during Au + Au (left plot) and $p+p$ run (right plot). Error bars are the RMS of vertex distribution.

3.3.2 Magnetic Field Stability

The best way to check the stability of magnetic field in central spectrometers is to check the particle average momentum. The figure 3.7 shows the average momentum for each run number in Au + Au and $p+p$ periods. The requirements to accept a run number were

- $0.55 < \langle P \rangle < 0.7 \text{ GeV}/c$ during Au + Au run

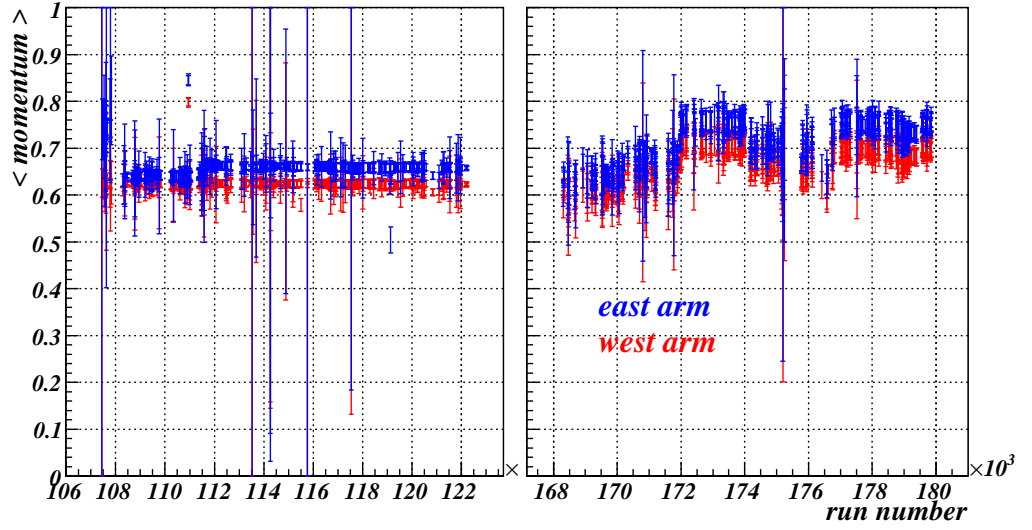


Figure 3.7: Average momentum of all charged particles in east and west spectrometer arms *versus* run number during Au + Au and $p+p$ collision periods. All tracks have hits in three DCH planes and matches PC1 and EmCal clusters.

- $0.55 < \langle P \rangle < 0.8 \text{ GeV}/c$ during $p+p$ run

During Au + Au period 94 run numbers, corresponding to 29.8M events, were rejected due to magnetic field problems. During $p+p$ period no run was rejected. The raise of average momentum occur because of the beam shift in $Y - X$ plane. The correction accounting this effect will be addressed in the section 3.4.1.

3.3.3 Electron Identification parameters check.

For electron identification QA we used only minimum bias events with $|Z \text{ vertex}| < 30\text{cm}$. We select tracks with at least

- two hits in X1, X2 DCH planes
- unambiguous hit at UV DCH plane
- association with a cluster in PC1
- $800 \text{ MeV}/c < \text{momentum} < 4.0 \text{ GeV}/c$

A run number is only accept for further analysis if all requirements bellow are obeyed :

RICH parameters using tracks with $\text{EmCal match} < 3\sigma_{pos}^{el}$, $dep > -2$ and subtracting Z swapped distributions ($sn0$, $s\chi^2/snpe0$, $sdis$)

- $\langle n0 \rangle > 3$

EmCal parameters using tracks with $n0 > 2$, $\chi^2/npe0 < 10$, and $disp < 5$ and subtracting Z swapped tracks in RICH ($sn0 > 2$, $s\chi^2/snpe0 < 10$, $sdisp < 5$)

- $|\langle emcsdphi_e \rangle| < 0.6$
- $|\langle emsdz_e \rangle| < 0.6$
- $-0.8 < \langle dep \rangle < 0.1$

3.3.4 Acceptance - Efficiency check.

During final yield calculation we need values for the detector acceptance and measure efficiency. This estimation is presented at the next chapter. But, if we want reliable efficiencies numbers we need to measure the fluctuation of this quantities and keep them under control. In this step of our QA we check

the constancy of electron production during the acquisition.

We used only minimum bias events with $|Z \text{ vertex}| < 30\text{cm}$ and selected electron candidates by using a tight criteria :

- two hits in X1, X2 DCH planes
- unambiguous hit at UV DCH plane
- association with a cluster in PC1
- $200\text{MeV}/c < p_T < 4\text{GeV}/c$
- $n0 \geq 3$
- $\chi^2/npe0 < 20$
- $disp < 5$
- $emcsdphi_e < 2$
- $emsdz_e < 2$

The *dep* distribution obtained (Fig.3.4) has Z swapped distribution subtracted as described in section 3.2. A Landau+Gaussian function is fitted to the remaining distribution. The integral of Gaussian component centered at zero give us the number of electrons.

The top plots in the figure 3.9 show the electron yield for each run accepted in section 3.3.3. The big jumps in electron yield correspond to periods

with known additional material installed on the beam pipe for electron conversion estimation. These periods are discarded in our analysis.

Since most of heavy vector mesons have electron and positrons going to different arms, it is more convenient we use the product of east and west arm yields as a selection criteria. The run dependence of this quantity is shown in the bottom plots of figure 3.9. The run numbers were grouped according to their yield and acquisition period. For each one of these groups was obtained a average number of electrons per minimum bias event and standard deviation. Only run numbers with yield matching in two sigmas it corresponding average number group were accept.

3.3.5 QA Summary

The table 3.2 shows the data set for heavy vector mesons analysis after quality selection.

specie	group	raw triggered events ($\times 10^6$)	recorded events ($\times 10^6$)
Au + Au	G3	119.4	85.0
	G4	34.6	17.7
	G5	224.4	158.6
	G6	89.0	62.2
	G7	195.5	144.7
	G8	168.4	118.4
	G9	290.8	215.2
	G10	458.5	330.7
	G11	136.4	95.6
TOTAL		1715	1229
$p+p$	G1		
	G2		
	G3		
	G4		
TOTAL			

Table 3.2: Data set after quality selection.

3.4 Parameters Calibration

3.4.1 Momentum

3.4.2 RICH Mirror Alignment

3.4.3 EmCal matching

3.4.4 dep

3.5 Electron Selection Optimization.

In this section our goal is obtain the most prominent J/ψ signal \mathcal{S} above the background \mathcal{B} . We use the signal significance

$$signal\ significance = \frac{\mathcal{S}}{\sqrt{\mathcal{S} + \mathcal{B}}} \quad (3.4)$$

We decided to use only parameters relying in the broader Cherenkov ring area ($3.8\text{ cm} < R < 11\text{ cm}$). The parameters χ^2 and *disp* were not used since they are calculated considering the tighter ring area. The optimization is performed with Au + Au data for 10 different event centrality regimes. The minimum track requirement set is :

- $|Z\ vertex| < 30\text{cm}$
- $dep > -4$
- $n1 \geq 2$
- $|emcsdphi_e| < 4$ and $|emcsdz_e| < 4$

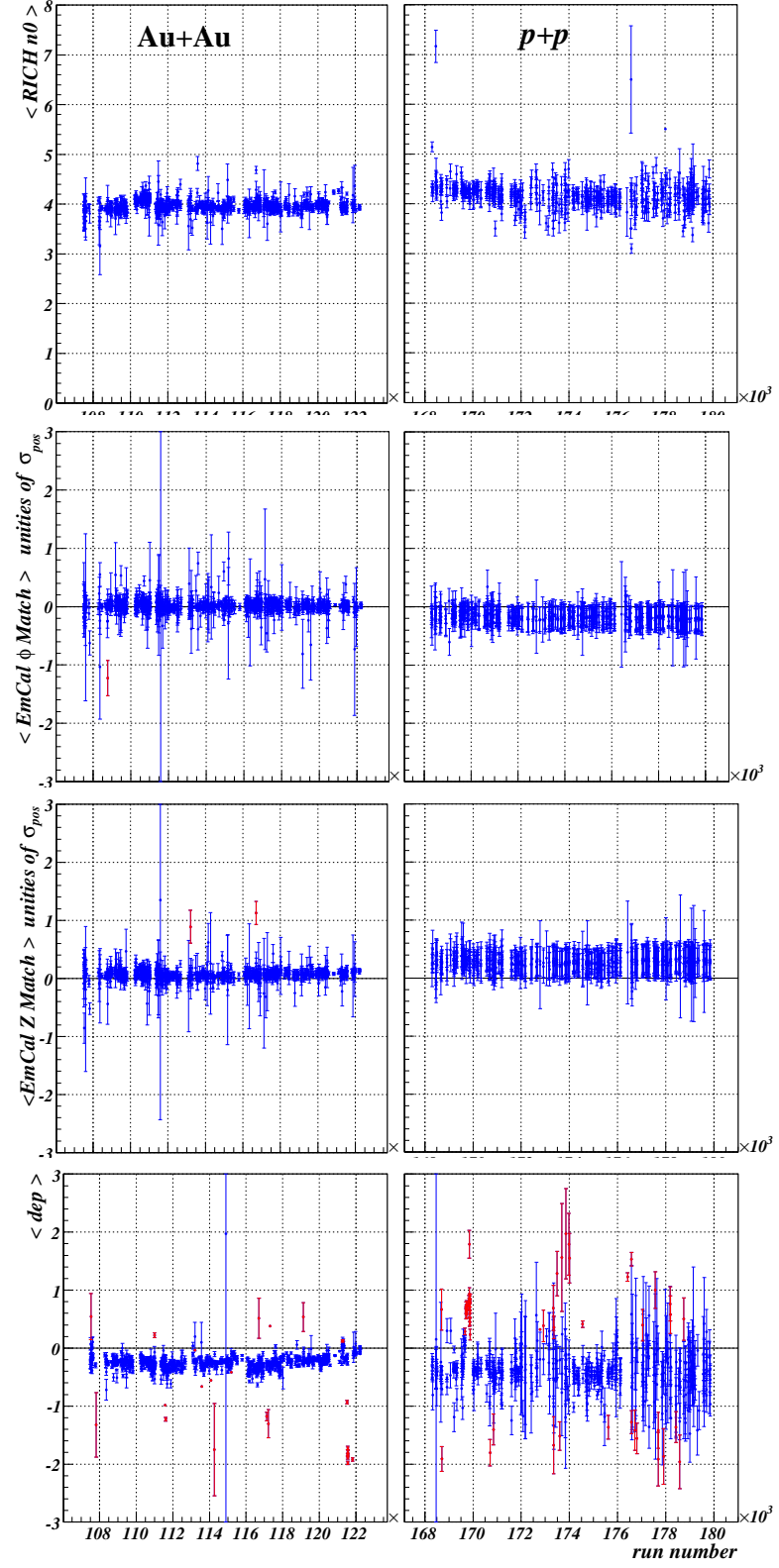


Figure 3.8: Run number dependences of electron identification parameters used in heavy vector mesons analysis. The red points are run number rejected for further analysis.

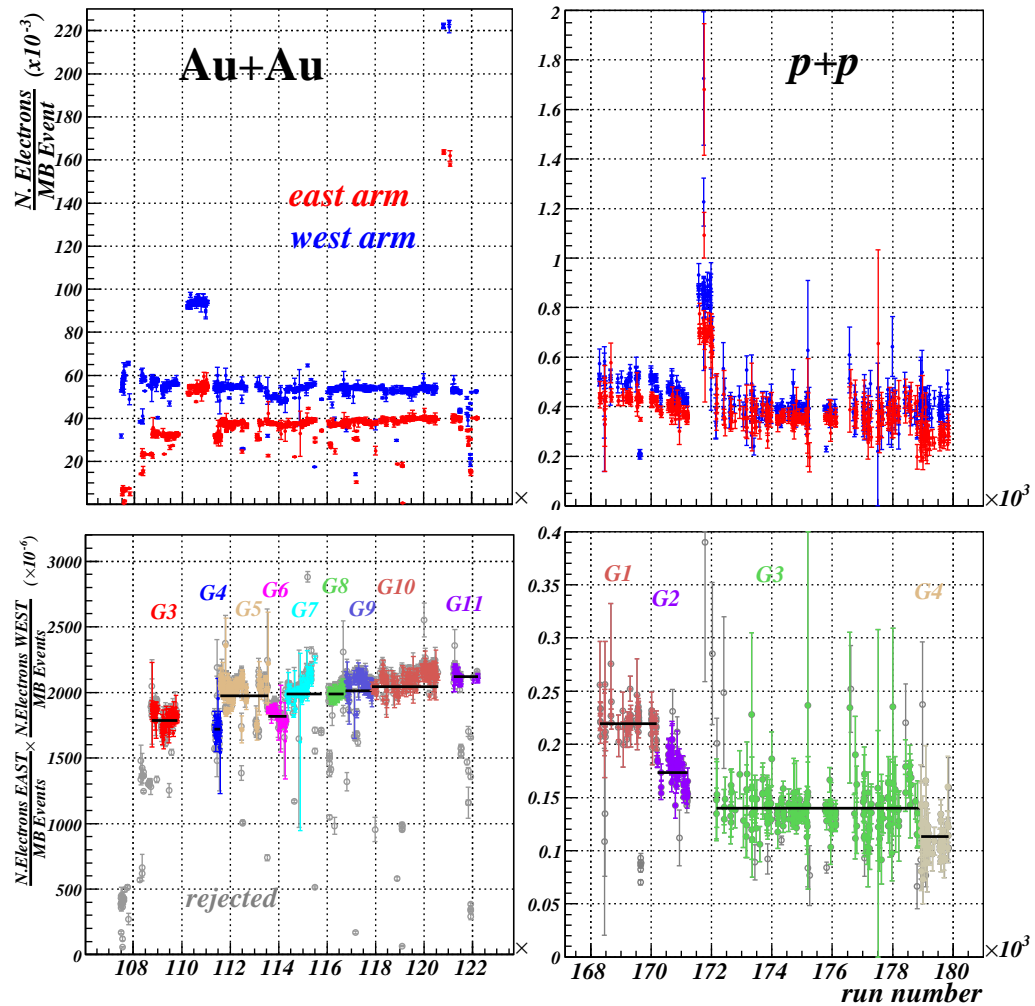


Figure 3.9: Run dependence of electron yield. The top panels show yields for each spectrometer arm. The bottom panels show the product obtained from both arms. The Au + Au and $p+p$ runs were split in acceptance groups. The horizontal lines are the average of each group. Gray open circles correspond to rejected runs.

Chapter 4

Acceptance and Efficiency Estimation.

4.1 PHENIX Monte Carlo Simulation : PISA

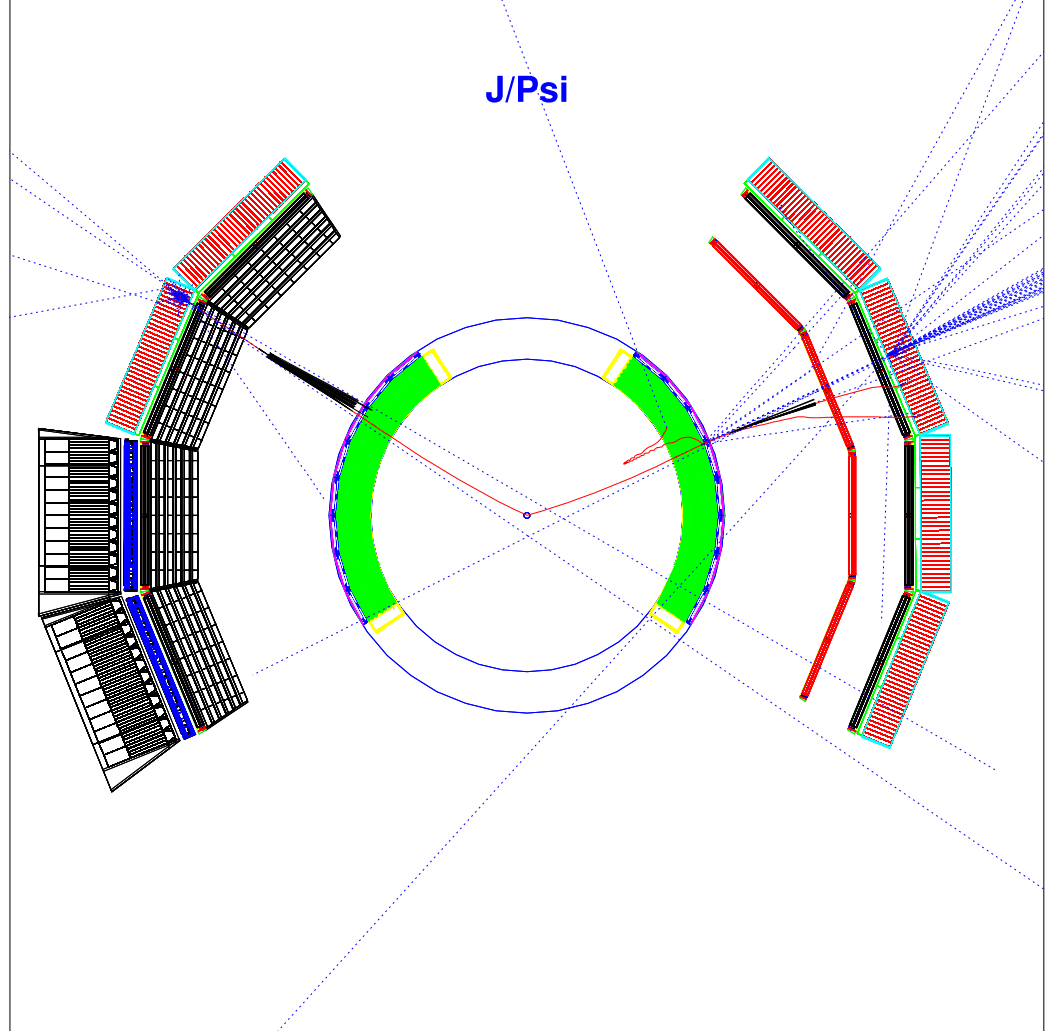


Figure 4.1: PHENIX Monte Carlo setup and the response to a generated J/ψ . Electrons are represented by red lines. Cherenkov photons are black lines. RICH structure is not drawn for clarity.

The Phenix Integrated Simulation Application (PISA) is a GEANT3 [1]

based simulation code, and has been successfully used since 1992 to answer many diverse questions about the expected performance of the PHENIX detector system. It tracks particles produced by event generators according to the PHENIX geometry and material installed (Fig. 4.1). The output from PISA returns the detector response to the particle generated on every designed active area.

In a second step the hit output bank is translated to raw signal similar to what we find in real data. In this process it is introduced dead areas and efficiency parameters inherent to detector performance. The parametrization of this process is described in section 4.3. Lastly, the raw data can be reconstructed by the same code used to reconstruct real data.

4.2 Conversion Electrons.

The parameters tuning in our PISA simulation is a sensitive step of detector efficiency determination. We need to make the PISA most realistic as possible for the period we took the data. The best manner is use a clean and unbiased real sample for this. Unfortunately, the use of electron beam tests are not feasible for installed detectors. An alternative source of clean and unbiased electrons with reasonable signal are $\gamma \rightarrow e^+e^-$ conversion in the beam pipe.

Since the e^+e^- pair comes from a massless particle, its invariant mass should be zero and the plane formed by the pair should be parallel to the mag-

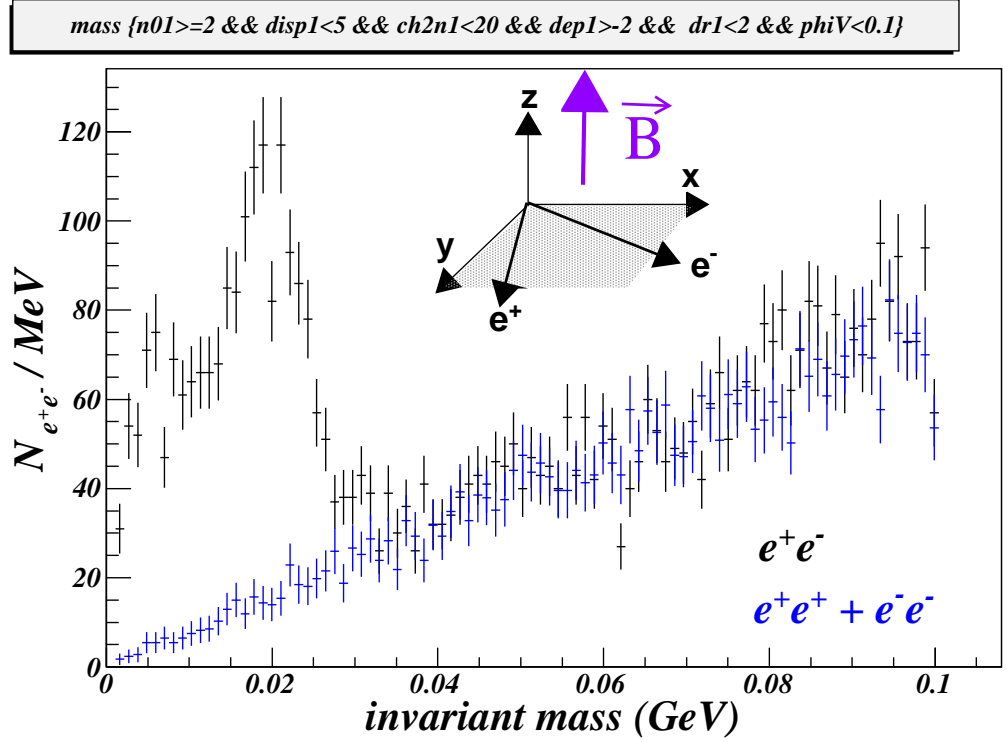


Figure 4.2: Invariant mass spectrum of $\gamma \rightarrow e^+e^-$ conversion in beam pipe.

netic field. But we have to consider the momentum obtained by the tracking algorithm for those electrons is scaled by a factor $R_{beam\ pipe}/R_{DCH} = 1.7\%$ ($R_{beam\ pipe} = 3.81cm$ and $R_{DCH} = 220cm$).

We can see this signal in the invariant mass spectrum close to zero (fig. 4.2) when we apply electron identification criteria for one of the particles of the pair. Once all conditions are satisfied, the second particle of the pair is an electron obtained without any identification criteria. We use this electron for simulation tuning (section 4.3) and efficiency estimation (section 4.5).

4.3 Tuning the PISA

4.3.1 eID Tuning

4.3.2 Dead Areas Implementation

4.4 J/ψ Acceptance \times Efficiency Calculation

4.5 Particle Multiplicity Dependence

Chapter 5

Measurement of J/ψ Production.

Chapter 6

Results Interpretation.

Bibliography

- [1] *GEANT User's Guide, 3.15*. CERN Program Library.
- [2] L. Aphecetche et al. Phenix calorimeter. *Nucl. Instrum. Meth.*, A499:521–536, 2003.